Supporting Information for "No detectable inflection point in U.S. oil and gas methane emissions following the Inflation Reduction Act"

Ao Chen[1*], William S. Daniels[1], Ziting Huang[1], Arvind P. Ravikumar[2], Sarah M. Jordaan[3], Zhen Zhang[4], Leyang Feng[1], Hanyu Liu[1], Lee T. Murray[5], Xueying Yu[6], Dylan C. Gaeta[1], Kristan L. Morgan[1], Jialuo Yuan[7], Scot M. Miller[1*]

[1]Department of Environmental Health and Engineering, Johns Hopkins University, Baltimore, MD, 21205, USA.
[2]Hildebrand Department of Petroleum and Geosystems Engineering, The University of Texas at Austin, Austin, TX, 78712, USA.
[3]Department of Civil Engineering, McGill University, Montreal, Quebec, H3A 0C3, Canada.
[4]National Tibetan Plateau Data Center (TPDC), State Key Laboratory of Tibetan Plateau Earth System, Environment and Resource (TPESER), Institute of Tibetan Plateau Research, Chinese Academy of Sciences, Beijing, 100101, China.
[5]Department of Earth and Environmental Sciences, University of Rochester, Rochester, NY, 14627, USA.
[6]Atmospheric Sciences Research Center, State University of New York at Albany, Albany, NY, 12226, USA.
[7]Department of Civil and Environmental Engineering, Stanford University, Stanford, CA, 94305, USA.

*Corresponding author(s). E-mail(s): achen152@jh.edu; smill191@jhu.edu;

Supplementary discussion

Sensitivity analysis of OH

Methane simulations in GEOS-Chem use archived OH fields that were previously generated from full chemistry simulations. By default, we use these archived fields in our study, as has been done in multiple previous studies [1, 2]. Several recent studies report that global OH mixing ratios changed by 1.6 – 4.0% in 2020 due to the COVID-19 pandemic, a variation not accounted for in the archived OH fields [3–6].

We further assess the impact of OH biases by reducing global OH fields by 1.6% – 4.0% in our regional inversion model, following recent constraints [3, 5]. In these sensitivity scenarios, total CONUS emissions decrease slightly from the baseline (scenario 3 in Table 1) from 56.8 Tg year^{-1} to between 55.9 and 56.4 Tg year^{-1}. This deviation of only 0.7%–1.5% confirms that our regional emission estimates are largely insensitive to global OH uncertainties within this range.

Uncertainty analysis and limitations

Our study is subject to several uncertainties and limitations. First, our ensemble detection limit is ∼0.35 Tg yr^{-1} (defined as 2σ of the ensemble variability) or ∼0.60 Tg yr^{-1} (defined as the full ensemble range width). Thus, we cannot rule out a counterfactual scenario where emissions would have risen more in the absence of the IRA. Hence, the observed absence of a detectable break may represent a "mitigated growth" rather than a policy failure. For ∼0.35 Tg yr^{-1}, we define the detection threshold ($\mathcal{L}_{det}$) as twice the standard deviation (2σ) of the ensemble. We take the standard deviation of the ensemble and multiply that number by 1.96 (or 2), analogous to a 95% confidence interval, and we cannot rule out a change in emissions smaller than this detection limit.

$$\mathcal{L}_{det} = 2\sigma = 2 \times \sqrt{\frac{1}{N-1}\sum_{i=1}^{N}(\Delta E_i - \overline{\Delta E})^2} \tag{S1}$$

where N represents the number of ensemble members ($N = 8$ in this study), ΔE_i denotes the year-over-year change in CONUS O&G methane emissions for the year-2024 compared to 2023 ($\Delta E_i = E_{2024,i} - E_{2023,i}$) for the i-th scenario, and $\overline{\Delta E}$ is the ensemble mean of these year-over-year emission changes.

For ∼0.60 Tg yr^{-1}, we define the conservative detection threshold ($\mathcal{L}_{det}$) as the full width of the ensemble range (maximum minus minimum):

$$\mathcal{L}_{det} = \max_{i=1}^{N}(\Delta E_i) - \min_{i=1}^{N}(\Delta E_i) \tag{S2}$$

where N represents the number of ensemble members ($N = 8$ in this study), and ΔE_i denotes the year-over-year change in CONUS O&G methane emissions ($\Delta E_i = E_{2024,i} - E_{2023,i}$) for the i-th scenario. This threshold represents the conservative envelope of structural uncertainty for distinguishing a physical trend from inverse model noise.

Second, we present the ensemble range of these 8 scenarios in the results, but we note that this ensemble range is not the same as the posterior uncertainties. We rely on the ensemble range rather than the posterior error covariance matrix ($\hat{\mathbf{S}}$) or Monte Carlo simulations due to computational considerations. The L-BFGS method is an efficient optimization algorithm that we can use to estimate millions of unknown emissions points in the inverse model, but it does not provide a mathematical estimate of the posterior uncertainty. An alternative approach to the uncertainties would be to generate a large number of Monte Carlo simulations, but this approach is precluded by computational constraints; a single year of our inverse modeling simulations with GEOS-Chem typically requires 25 days of computing time and approximately 100 GB of storage. Scaling this simulation to 100 Monte Carlo simulations would demand prohibitive memory (over 10 TB per year) and time (approximately 2500 days if run sequentially), making it impractical for our analysis with the GEOS-Chem adjoint model. While algorithms exist to calculate posterior uncertainties without additional simulations [7], the current flexibility of the GEOS-Chem adjoint model limits their immediate implementation. Consequently, we utilize the ensemble range to calculate the uncertainty. An upside of this approach is that we are able to evaluate the effect of different model configurations on the emissions estimate (e.g., different covariance matrix parameters, different constructions of the prior), something that traditional posterior uncertainty estimates do not capture.

Third, the attribution of emissions to specific sources introduces additional uncertainty in the posterior estimates. Specifically, our approach relies on the relative ratio of anthropogenic versus wetland emissions in prior bottom-up inventories; consequently, errors in this partitioning could propagate into the estimated source attribution. Importantly, however, this attribution method implies that our results depend on the relative magnitude of the emissions inventories used as predictor variables in the inverse model rather than their absolute magnitudes [8].

Beyond these uncertainties, the consistency (or inconsistency) of TROPOMI data coverage is an additional concern. TROPOMI generally provides over 500 valid observations per 0.5° latitude by 0.625° longitude grid box per season across most of our CONUS domain. However, we do see some spatial heterogeneity in observational coverage (see Fig. S5 – S6). An important caveat is the reduced observation density in the Northwestern U.S. (e.g., Washington, Oregon, Idaho, and Montana) during winter and spring, driven by persistent cloud cover. This seasonality limits the inverse model's sensitivity to emission changes in these regions during colder months.

Current status and uncertainty of the IRA

Although many rules and grants under the IRA have officially been implemented, political turnover in Washington creates uncertainty about their long-term enforcement and funding, suggesting that the full methane emissions reductions have likely not yet been realized. Specifically, the IRA introduced a waste emissions charge on methane emissions from the oil and gas sector, setting a fee of $900 per metric ton starting in 2024, increasing to $1,200 in 2025, and $1,500 in 2026 and beyond [9]. This fee was finalized but was just beginning to be implemented in 2024; however, a joint Congressional resolution disapproved the Final Waste Emissions Charge Rule on March

14, 2025. This disapproval, enacted as Public Law 119-2 on March 14, 2025, prevents the WEC from taking effect and triggers a statutory prohibition against issuing any "substantially the same" regulation in the future, thereby leaving the WEC without an enforceable implementation mechanism despite the underlying statutory mandate [10].

The IRA also launched the Climate Pollution Reduction Grants program, offering nearly $5 billion to state and local governments for projects like landfill methane gas capture (https://www.epa.gov/inflation-reduction-act/cprg-selected-applications-sector-waste-and-materials-management) [11]. The IRA further established the Methane Emissions Reduction Program, allocating $1.36 billion to provide technical and financial support to the oil and gas sector. (https://www.epa.gov/inflation-reduction-act/methane-emissions-reduction-program) [12]. Specifically, this program offers $850 million to help small oil and gas operators cut methane emissions and $350 million to 14 states for voluntary well plugging [12]. Although some funding ($350 million has been awarded, the IRA's full impact on U.S. methane emissions remains unclear and depends on ongoing support.

Several additional voluntary international agreements and regulations in numerous states could also help reduce U.S. methane emissions. Several states have established methane (or greenhouse gas) emissions reduction targets, summarized in Table S2. In addition, the U.S. has joined the Global Methane Pledge, committing to a 30% reduction in methane emissions by 2030 compared to 2020 levels [13]. However, the Global Methane Pledge is voluntary and not a binding U.S. domestic law. Note that the U.S. officially withdrew from the Paris Agreement on January 27, 2026 [14] and has effectively abandoned the Global Methane Pledge by repealing federal implementation mechanisms (e.g., the WEC) .

More details of the L-BFGS method

We estimate the emissions ($\boldsymbol{s}$) and coefficients ($\boldsymbol{\beta}$) simultaneously by minimizing the following equation:

$$L(\boldsymbol{s},\boldsymbol{\beta}) = \frac{1}{2}(\boldsymbol{z}-\boldsymbol{h}(\boldsymbol{s}))^\top \mathbf{R}^{-1}(\boldsymbol{z}-\boldsymbol{h}(\boldsymbol{s})) + \frac{1}{2}(\boldsymbol{s}-\mathbf{X}\boldsymbol{\beta})^\top \mathbf{Q}^{-1}(\boldsymbol{s}-\mathbf{X}\boldsymbol{\beta}) \tag{S3}$$

$$L(\boldsymbol{s}^*,\boldsymbol{\beta}) = \frac{1}{2}(\boldsymbol{z}-\boldsymbol{h}(\boldsymbol{s}^*\odot\boldsymbol{s}^*))^\top \mathbf{R}^{-1}(\boldsymbol{z}-\boldsymbol{h}(\boldsymbol{s}^*\odot\boldsymbol{s}^*)) + \frac{1}{2}(\boldsymbol{s}^*\odot\boldsymbol{s}^*-\mathbf{X}\boldsymbol{\beta})^\top \mathbf{Q}^{-1}(\boldsymbol{s}^*\odot\boldsymbol{s}^*-\mathbf{X}\boldsymbol{\beta}) \tag{S4}$$

where $L(\boldsymbol{s},\boldsymbol{\beta})$ is the objective function to minimize. The transformation $\boldsymbol{s} = \boldsymbol{s}^* \odot \boldsymbol{s}^*$ is employed to enforce the non-negativity constraint on the state vector $\boldsymbol{s}$, where $\odot$ denotes the Hadamard product (element-wise multiplication). By parameterizing the objective function in terms of $\boldsymbol{s}^*$, the original constrained optimization problem is mapped into an unconstrained space, as $(s_i^*)^2 \geq 0$ is guaranteed for any $s_i^* \in \mathbb{R}$. We minimize this objective function using the Limited-memory Broyden-Fletcher-Goldfarb-Shanno (L-BFGS) algorithm [15]. In our case, the number of observations n and the number of variables m to optimize are very large, so we use L-BFGS instead of BFGS because L-BFGS can handle high-dimensional problems efficiently without large memory requirements.

Supplementary tables

Table S1 Timeline of U.S. methane regulations (2012–2026), including NSPS OOOO, OOOOa, OOOOb, EG OOOOc [16], Policy Rule Rollback [17].

Year	Instrument	Legal Basis	Summary
2012 (Obama)	NSPS OOOO	Clean Air Act (CAA) §111(b)	Did not regulate methane directly. Regulated VOCs from new sources from August 23, 2011 to September 18, 2015.
2016 (Obama)	NSPS OOOOa	CAA §111(b)	Methane Added. Regulated methane from new sources from September 18, 2015 to December 6, 2022.
2020 (Trump)	Policy Rule Rollback	Executive Action	Rescission. Removed methane-specific requirements.
2021 (Biden)	Congressional Review Act Resolution	Legislative	Reinstatement. Congress nullified the 2020 rollback, instantly restoring NSPS OOOOa.
2022 (Biden)	Inflation Reduction Act	CAA §136	WEC Established. Created the methane fee. Exemptions are legally tied to future compliance with EPA rules (specifically SIPs).
2024 (Biden)	NSPS OOOOb	CAA §111(b)&(d)	Regulated methane from new sources after December 6, 2022.
2024 (Biden)	EG OOOOc	CAA §111(b)&(d)	The Critical Gap. OOOOc requires states to submit SIPs by March 2026. However, No state submitted a SIP in 2024, so the "Regulatory Compliance Exemption" for WEC was technically inaccessible.
2025 (Trump)	Repeal of WEC	Legislative	WEC and SIP termination. The WEC is repealed before the SIP deadline (2026). The exemption mechanism was never utilized.
2026 (Trump)	Endangerment Finding Revoked	Executive Order	Legal Void. Withdrawal of the health finding voids the legal basis for all NSPS and EG rules.

Table S2 Statutory methane (or greenhouse gas) emissions reduction targets of each state [18]

State	Target
United States	The U.S. has agreed to reduce methane emissions by 30% by 2030, compared to 2020 levels, under the Global Methane Pledge (voluntary).
California	By 2030, California aims to reduce methane by 40% compared to 2013 levels, under the SB 1383.
Colorado	Colorado aims to cut greenhouse gas emissions by 26% by 2025, 50% by 2030 and 90% by 2050 from 2005 levels under HB 19-1261.
Connecticut	Connecticut, under Public Act 18-82, targets greenhouse gas emissions reductions of 10% by 2020 (1990 baseline), and 45% by 2030 and 80% by 2050 (2001 baseline).
Delaware	Delaware plans to reduce greenhouse gas emissions, including methane, by 50% by 2030, compared to 2005 levels, under HB 99.
Hawaii	Hawaii plans to achieve a zero-emissions economy no later than 2045,under HB 2182.
Maine	By 2030, Maine aims to reduce greenhouse gas emissions, including methane, by 45% compared to 1990 levels.
Maryland	Maryland plans to reduce greenhouse gas emissions, including methane, by 25% by 2020 and 40% by 2030, compared to 2006 levels.
Massachusetts	By 2050, Massachusetts aims to reduce greenhouse gas emissions, including methane, by 85% compared to 1990 levels, under SB 9.
Minnesota	Minnesota aims to reduce greenhouse gas emissions by 30% by 2025, compared to 2005 levels.
Nevada	Nevada plans to cut greenhouse gas emissions, including methane, by 28% by 2025, compared to 2005 levels, and by 45% by 2030, under SB 254.
New Jersey	By 2050, New Jersey plans to reduce greenhouse gas emissions, including methane, by 80% compared to 2006 levels, under the Global Warming Response Act.
New Mexico	New Mexico aims to reduce greenhouse gas emissions, including methane, by 45% by 2030, compared to 2005 levels, under Executive Order 2019-003.
New York	New York plans to cut greenhouse gas emissions, including methane, by 40% by 2030, compared to 1990 levels, under the Climate Leadership and Community Protection Act.
North Carolina	North Carolina aims to cut greenhouse gas emissions, including methane, by 40% by 2030, compared to 2005 levels under Executive Order 80.
Oregon	Oregon plans to reduce greenhouse gas emissions, including methane, by 10% by 2020, compared to 1990 levels, and by 75% by 2050, under HB 3543.
Rhode Island	By 2020, Rhode Island aims to cut greenhouse gas emissions, including methane, by 10% compared to 1990 levels, and by 45% by 2035, under the Resilient Rhode Island Act of 2014.
Vermont	Vermont plans to reduce greenhouse gas emissions, including methane, by 40% by 2030, compared to 1990 levels, and by 80% by 2050, under HB 688.
Virginia	Virginia aims to achieve net-zero greenhouse gas emissions by 2045, including methane, under SB 94.
Washington	Washington plans to reduce greenhouse gas emissions, including methane, by 45% by 2030, compared to 1990 levels, and by 95% by 2050, under HB 2311.

Supplementary figures

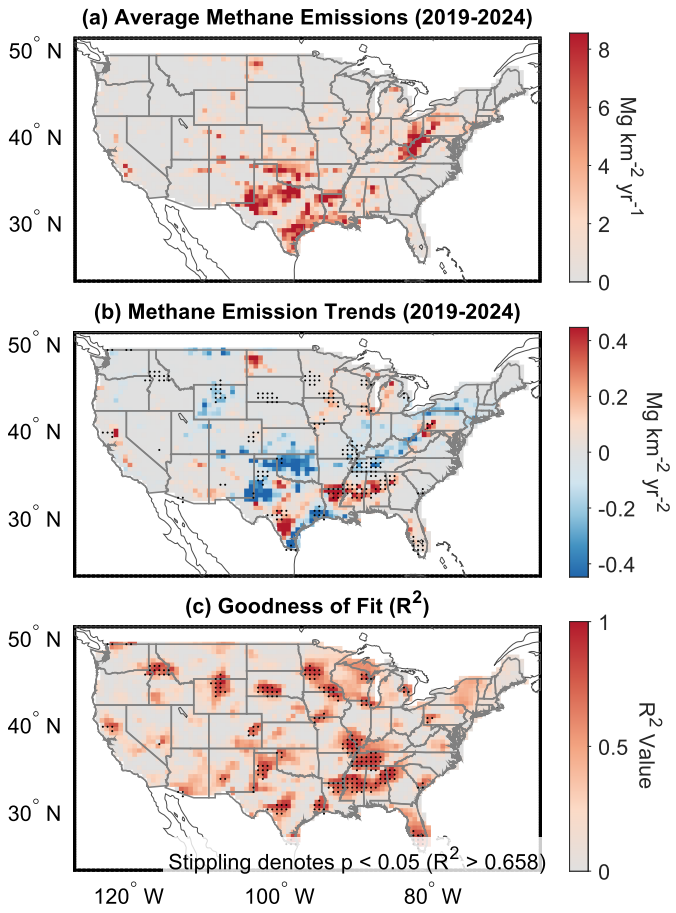

Fig. S1 Spatial distribution of U.S. O&G methane emissions, linear emission trends, and R-squared value of the trend during 2019–2024. Panel (a) presents the multi-year average O&G methane emissions per grid (Mg km^{-2} yr^{-1}) for 8 scenarios. Panel (b) shows the pixel-wise linear emission trends calculated over the six-year period (Mg km^{-2} yr^{-2}). Panel (c) displays the goodness of fit (R-squared value) for the linear regression at each corresponding grid cell. The grid marked by black dots in the panels (b) and (c) denotes regions with statistically significant trends ($p < 0.05$), which mathematically corresponds to an R-squared value greater than 0.658 for the 6-year sample size. Areas outside the CONUS are masked out.

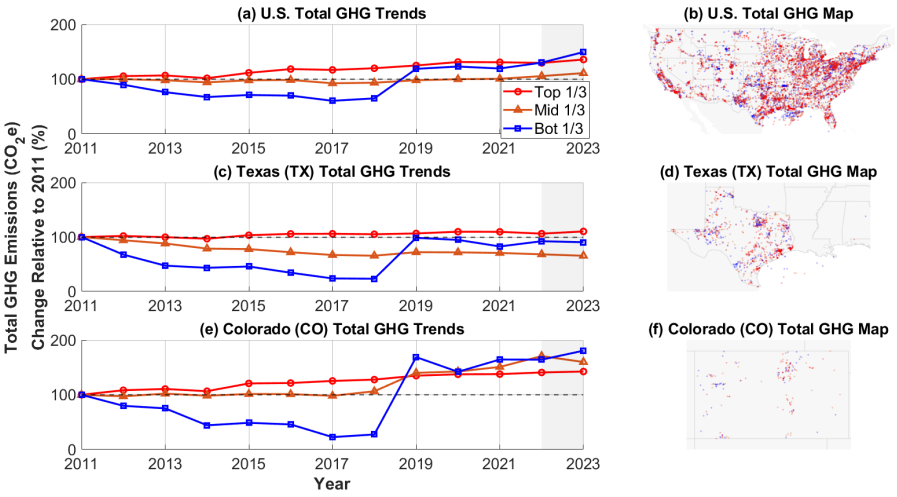

Fig. S2 Trends and geographic distribution of reported GHG from the onshore O&G Production sector in the U.S., Texas, and Colorado from EPA GHGRP during years 2011–2023. Annual GHGRP onshore O&G GHG emissions relative to 2011 levels for facilities grouped by their average emission magnitude: Large (Top 1/3), Medium (Middle 1/3), and Small (Bottom 1/3) for (a) U.S. (c) Texas, and (e) Colorado. Facility locations colored by group in the (b) U.S. (d) Texas, and (f) Colorado. Note that facilities emitting less than 25,000 t CO_2e are exempt for GHGRP and are not shown here.

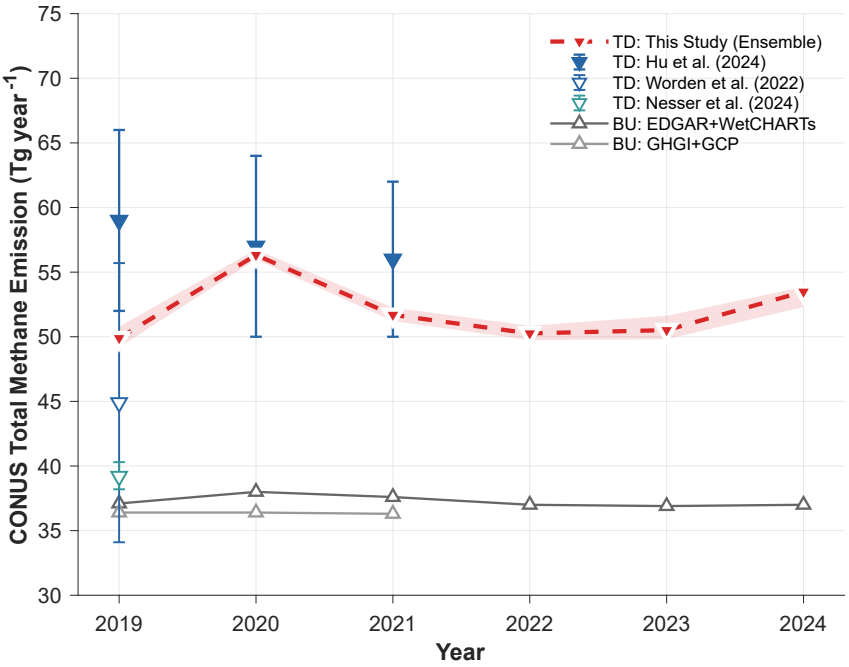

Fig. S3 Total methane emission estimates from CONUS during 2019–2024. The figure presents a comprehensive comparison between our top-down estimates and previous work. Up-pointing triangles represent bottom-up (BU) inventory-based estimates (EDGAR+WetCHARTs and GHGI+GCP). Down-pointing triangles denote top-down (TD) inversion results from this study (red dashed line) and previous work, including Hu et al. [19], Worden et al. [20], and Nesser et al. [21]. Vertical bars represent the reported uncertainty or min–max ranges. Our results consistently show higher methane levels compared to official inventories, aligning with recent observation-based findings.

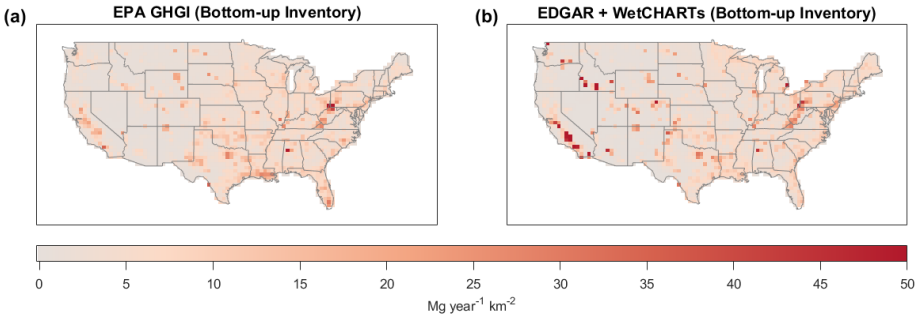

Fig. S4 Spatial distribution of bottom-up methane emission inventories (2019–2024) used as predictor variables in the inverse model. Panels show total methane emission (Mg yr^{-1} km^{-2}) derived from (a) EPA + GCP and (b) EDGAR + WetCHARTs. These inventories are used in $\mathbf{X}$ matrix in our inverse model.

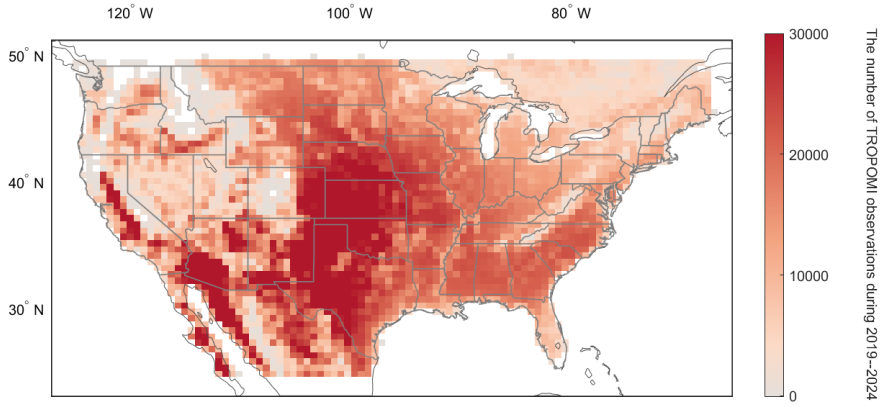

Fig. S5 The number of satellite observations (the blended TROPOMI + GOSAT satellite data) during 2019–2024 at a 0.5° latitude by 0.625° longitude grid resolution.

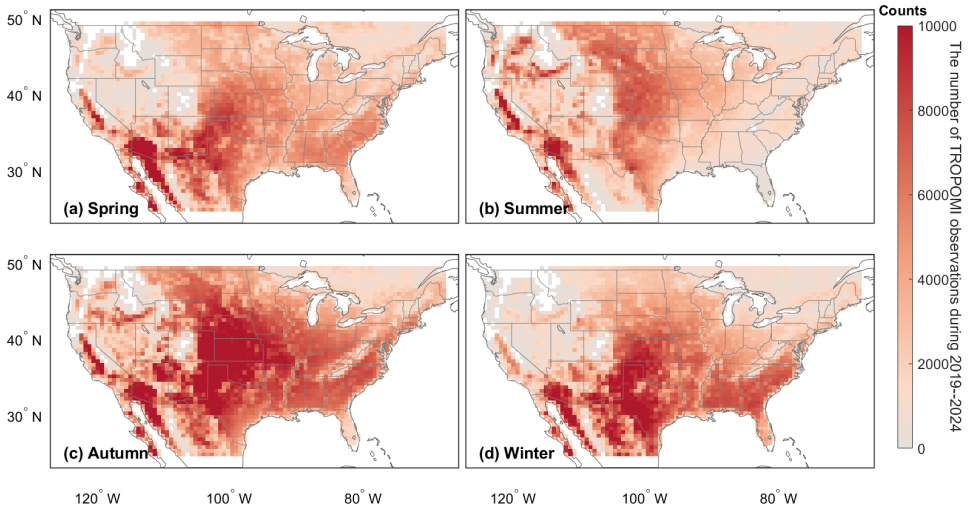

Fig. S6 The number of satellite observations (the blended TROPOMI + GOSAT satellite data) for each season during 2019–2024 at a 0.5° latitude by 0.625° longitude grid resolution. Seasons for each grid cell are defined as spring (March–May), summer (June–August), autumn (September–November), and winter (December–February).

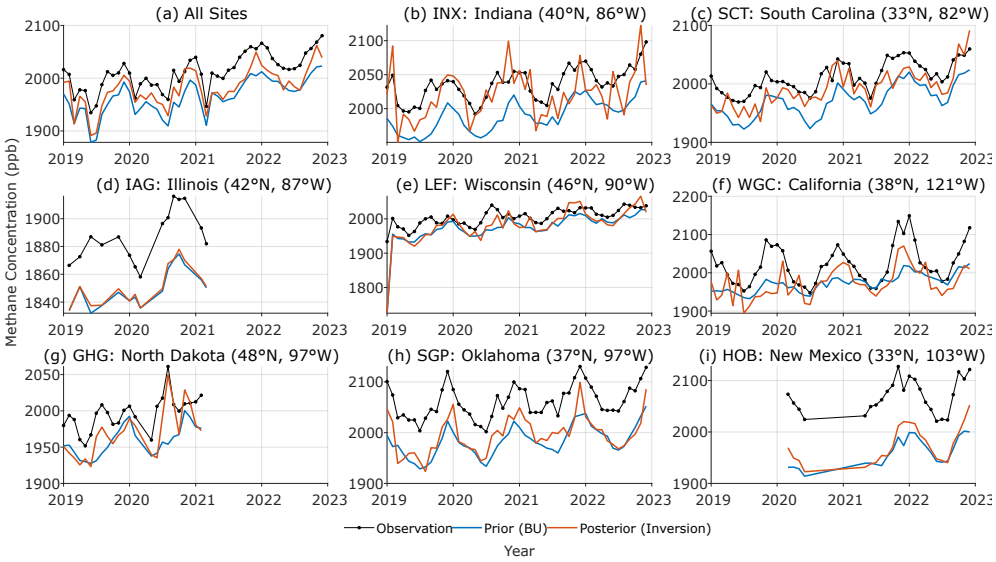

Fig. S7 Monthly mean average of GEOS-Chem (GC) output using posterior emissions (red line), bottom-up emissions (blue line), and in-situ observations (black line), from (a) all in-situ data (Note that we simply averaged all the data for each month and did not weight them by region.), (b) INX, Indiana, USA (40°N, 86°W), (c) SCT, South Carolina, USA (33°N, 82°W), (d) IAG, Illinois, USA (42°N, 87°W), (e) LEF, Wisconsin, USA (46°N, 90°W), (f) WGC, California, USA (38°N, 121°W), (g) GHG, USA (48°N, 97°W), (h) SGP, Oklahoma, USA (37°N, 97°W), and (i) HOB, New Mexico, USA (33°N, 103°W). In this figure, bottom-up emissions refers to the mean of the GCP models plus EDGAR plus other emissions sources from HEMCO. Statistical metrics, including the Pearson correlation coefficient (R), Root Mean Square Error (RMSE), Mean Bias Error (MBE), and Mean Absolute Error (MAE), are provided for both prior and posterior simulations. All data are filtered within the range of 1800–2400 ppb.

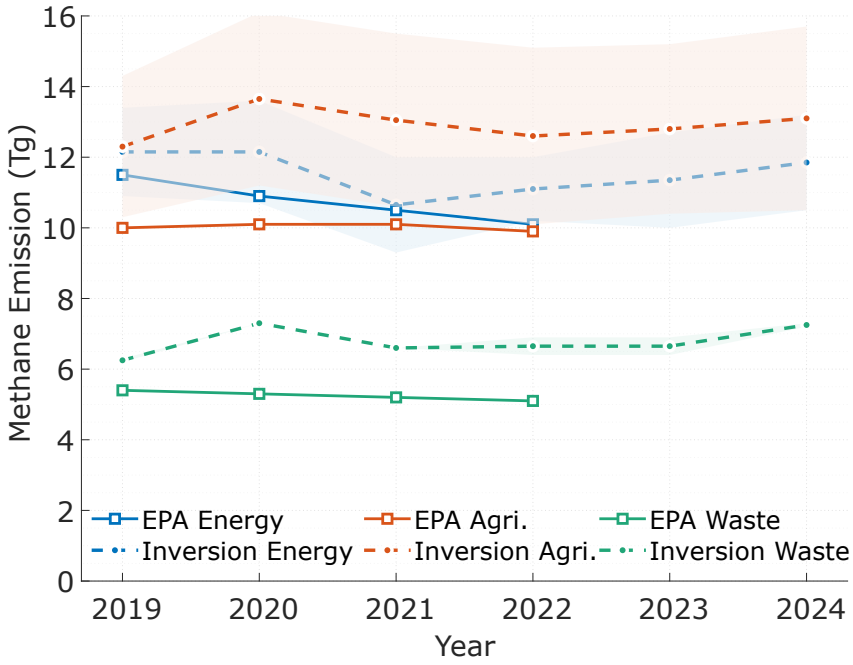

Fig. S8 Sectoral methane emissions in US for EPA GHGI versus inversion estimates. This figure compares bottom-up estimates (EPA, solid lines) with our top-down inversion estimates (dashed lines with uncertainty envelopes) across three key sectors, including energy (blue), agriculture (orange), and waste (green). The inversion results consistently suggest higher emissions than official inventories, with shaded regions representing the min–max range of the inversion ensemble.

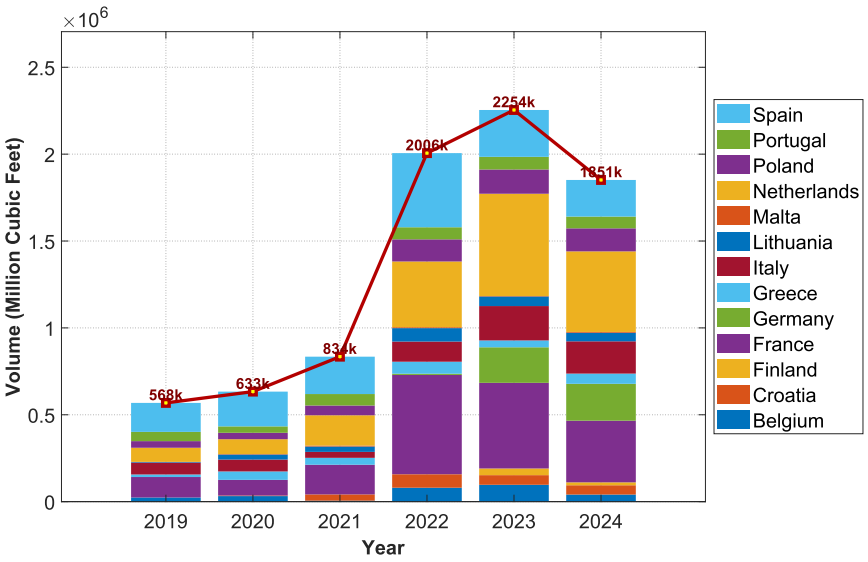

Fig. S9 U.S. Liquefied Natural Gas (LNG) export volumes to European Union member states during 2019–2024. This figure illustrates the significant surge in U.S. LNG exports to the European Union starting in 2022. Data processed from the U.S. Energy Information Administration [22] (EIA, 2025) Natural Gas Export Reports.

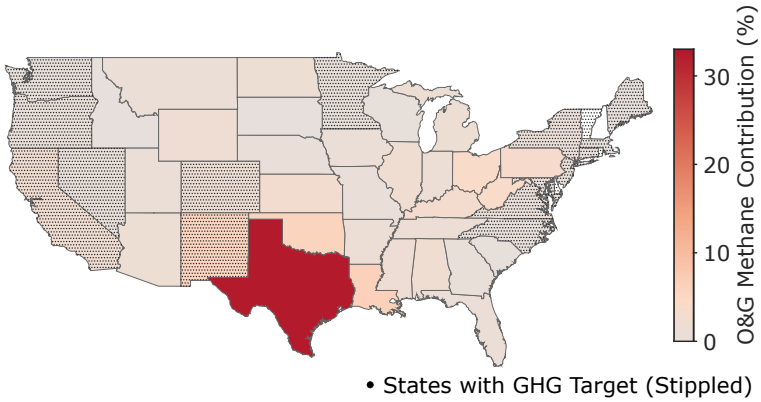

Fig. S10 State-level GHG reduction targets and contributions to U.S. O&G methane emissions. The base map illustrates each state's proportional contribution (%) to the total U.S. oil and gas methane emissions. Emission values are calculated as the absolute ensemble average across eight scenarios spanning the 2019–2024 period. States that have statutory GHG reduction targets are denoted by stippling (black dots).

References

[1] Thompson, R. L. *et al.* Methane fluxes in the high northern latitudes for 2005-2013 estimated using a Bayesian atmospheric inversion. *Atmospheric Chemistry and Physics* **17**, 3553–3572 (2017).

[2] Yu, X. *et al.* Aircraft-based inversions quantify the importance of wetlands and livestock for Upper Midwest methane emissions. *Atmospheric Chemistry and Physics* **21**, 951–971 (2021).

[3] Peng, S. *et al.* Wetland emission and atmospheric sink changes explain methane growth in 2020. *Nature* **612**, 477–482 (2022).

[4] Qu, Z. *et al.* Attribution of the 2020 surge in atmospheric methane by inverse analysis of GOSAT observations. *Environmental Research Letters* **17** (2022).

[5] Chen, W., Zhang, Y. & Liang, R. Converging evidence for reduced global atmospheric oxidation in 2020. *National Science Review* **12**, nwaf232 (2025). URL https://doi.org/10.1093/nsr/nwaf232.

[6] Ciais, P. *et al.* Why methane surged in the atmosphere during the early 2020s. *Science* **24**, 2026 (2026). URL https://www.science.org/doi/10.1126/science.adx8262.

[7] Cho, T., Chung, J., Miller, S. M. & Saibaba, A. K. Computationally efficient methods for large-scale atmospheric inverse modeling. *Geoscientific Model Development* **15**, 5547–5565 (2022).

[8] Chen, A. *et al.* Spatial and temporal distribution of global wetland methane emissions during 2019–2020 estimated from satellite observations. *Journal of Geophysical Research: Atmospheres* **130** (2025).

[9] EPA. Waste Emissions Charge (2025). URL https://www.epa.gov/inflation-reduction-act/waste-emissions-charge.

[10] Ramseur, J. L. Inflation Reduction Act Methane Emissions Charge: Overview and Developments. CRS Report R48475, Congressional Research Service (2025). URL https://www.congress.gov/crs-product/R48475.

[11] EPA. CPRG Selected Applications by Sector - Waste and Materials Management (2024). URL https://www.epa.gov/inflation-reduction-act/cprg-selected-applications-sector-waste-and-materials-management.

[12] EPA. Methane Emissions Reduction Program (2024). URL https://www.epa.gov/inflation-reduction-act/methane-emissions-reduction-program.

[13] Global Methane Pledge. Global Methane Pledge (2025). URL https://www.globalmethanepledge.org/news/open-letter-global-methane-pledge-endorsers.

[14] The White House. Fact Sheet: President Donald J. Trump Withdraws the United States from International Organizations that Are Contrary to the Interests of the United States (2026). URL https://www.whitehouse.gov/fact-sheets/2026/01/fact-sheet-president-donald-j-trump-withdraws-the-united-states-from-international-organizations-that-are-co Accessed: 2026-03-31.

[15] Liu, D. C. & Nocedal, J. On the limited memory BFGS method for large scale optimization. *Mathematical Programming* **45**, 503–528 (1989).

[16] National Archives. Code of Federal Regulations, Title 40, Protection of Environment, Part 60. Electronic Code of Federal Regulations (eCFR) (2026). URL https://www.ecfr.gov/current/title-40/chapter-I/subchapter-C/part-60. Accessed: March 27, 2026.

[17] Vizcarra, H. EPA's Final Methane Emissions Rules Roll Back Standards and Statutory Authority. Harvard Law School Environmental & Energy Law Program (EELP) Legal Analysis (2020). URL https://eelp.law.harvard.edu/epas-final-methane-emissions-rule-rolls-back-standards-and-statutory-authority/. Updated to reflect the publishing of rules in the Federal Register. Accessed: 2026-03-31.

[18] Shields, L. Greenhouse Gas Emissions Reduction Targets and Market-based Policies. National Conference of State Legislatures (NCSL) Report (2023). URL https://www.ncsl.org/energy/greenhouse-gas-emissions-reduction-targets-and-market-based-policies.

[19] Hu, L. *et al.* An unexpected seasonal cycle in U.S. oil and gas methane emissions. *Environmental Science & Technology* **59** (2025). URL https://pubs.acs.org/doi/10.1021/acs.est.4c14090.

[20] Worden, J. R. *et al.* The 2019 methane budget and uncertainties at 1° resolution and each country through Bayesian integration of GOSAT total column methane data and a priori inventory estimates. *Atmospheric Chemistry and Physics* **22**, 6811–6841 (2022). URL https://acp.copernicus.org/articles/22/6811/2022/.

[21] Nesser, H. *et al.* High-resolution US methane emissions inferred from an inversion of 2019 TROPOMI satellite data: contributions from individual states, urban areas, and landfills. *Atmospheric Chemistry and Physics* **24**, 5069–5091 (2024). URL https://acp.copernicus.org/articles/24/5069/2024/.

[22] U.S. Energy Information Administration. U.S. Natural Gas Exports and Re-Exports by Country. EIA Data Browser (2026). URL https://www.eia.gov/dnav/ng/ng_move_expc_s1_a.htm. Annual export volumes (Million Cubic Feet) for Pipeline (Canada, Mexico) and LNG during 1973–2025. Accessed: 2026-03-31.